Sustainable bio-hydrothermal sequencing treatment for asbestos-cement wastes

Simultaneous treatment of agro-food and asbestos-cement waste by the combination of dark fermentation and hydrothermal processes

Marco Race[a], Danilo Spasiano[b]*, Vincenzo Luongo[a], Andrea Petrella[b], Saverio Fiore[c], Francesco Pirozzi[a], Umberto Fratino[b], Alberto F. Piccinni[b]

[a] Dipartimento di Ingegneria Civile, Edile ed Ambientale, Università di Napoli Federico II, Via Claudio, 21, 80125, Napoli, Italy.

[b] Dipartimento di Ingegneria Civile, Ambientale, Edile, del Territorio e di Chimica, Politecnico di Bari, Via E. Orabona, 4, 70125, Bari, Italy.

[c] Institute of Methodologies for Environmental Analysis, National Research Council of Italy, Tito Scalo, Potenza, Italy.

* Corresponding Author: tel.: (+39) 0805963240; danilo.spasiano@poliba.it.

Abstract

The inadequate management of asbestos-cement products (ACP) and/or wastes (ACW) generates hazardous airborne dusts. For this reason, the EU is promoting the removal of ACP from utilities, public and private buildings and is looking for innovative ACW treatments alternative to the landfilling. The simultaneous treatment of ACW and orange pulp or cheese whey was attempted with a mesophilic dark fermentation (DF) process followed by a 12 h hydrothermal (HT) treatment carried out with the addition of lactic or oxalic acid at 100 °C and ambient pressure. The DF of orange pulp or cheese whey in the presence of 5 g L^{-1} ACW lasted 171 h and led to the production of 4 L_{H_2} and 5 L_{H_2} per litre of solution, respectively. During the DF, the dissolution of the ACW matrix was almost completed, and the partial collapse of the asbestos fibres was observed. Both the

organic acids that were added during the HT tests at a concentration ≥2.5 g L^{-1} completely destroyed the asbestos fibres. However, when 1.25 g L^{-1} lactic or oxalic acid was added before the HT tests, few fibre fragments were found, and their chemical composition differed from that of chrysotile.

Keywords: orange pulp; cheese whey; oxalic acid; chrysotile; hydrogen; asbestos-cement waste treatment.

1. Introduction

Chrysotile, also called white asbestos, is the most used type of asbestos, and it is considered to be a human carcinogen (Donaldson et al., 2013; Stayner et al., 2013). Chrysotile consists of sheets of $Mg(OH)_2$ (brucite-like sheets) bonded to sheets of SiO_2, and it is characterized by a layered structure that is wrapped around itself to form a tubular fibre structure with a spiral section (Falini et al., 2004). In a very recent paper, the adoption of the DF process as a pretreatment of an acid-infused HT phase was proposed to destroy the chrysotile fibres contained in ACW to save energy and reagents (Spasiano et al., 2017). Indeed, the biological DF treatment led to the conversion of glucose in CO_2- and H_2-rich biogas and organic acids (OA) (Saleem et al., 2018), which dissolved all of the calcium-based compounds from the cement matrix and part of the brucite-like sheets of the chrysotile fibres constituting the Eternit sample (Spasiano, 2018). Consequently, during the acid-infused HT treatment that was carried out at 100 °C under ambient pressure, the amount of sulfuric acid, which was required to completely dissolve the suspended brucitic layers was halved with respect to a previous finding (Nam et al., 2014). Similar results were obtained when 1.25 g L^{-1} malic or lactic acid was added instead of

the same amount of sulfuric acid, but in these cases, the anaerobic digestion (AD) of the HT effluents led to an additional source of energy in the form of bio-methane (Spasiano et al., 2019). Notably, besides to chemicals savings, this treatment train led to the production of both bio-hydrogen and bio-methane, which can energetically support the HT treatment. Consequently, the adoption of a DF stage followed by the HT and AD treatments could overcome the high energy and/or reagents requirement issues of the conventional ACW treatments (Spasiano and Pirozzi, 2017) and support the application of the recently introduced ACW treatment train at the industrial scale.

The above mentioned studies were carried out by adding glucose as a biodegradable substrate in a $[C_6H_{12}O_6]$/[ACW] mass ratio equal to 12 during the DF. Even if an aqueous solution of glucose could simulate the molasses produced by sugar refineries (Sen et al., 2019), the production is not enough to meet the needs of this treatment train, since the quantity of ACW to be disposed is very high. For example, the ACW to be treated in Italy and in Flanders, which is a Belgian region, equals 3.0×10^7 ton and 3.7×10^6 ton, respectively (OVAM, n.d.; Plescia et al., 2003). However, instead of glucose, other biodegradable substrates could be used during the DF, such as the organic fraction of municipal solid waste (Shin et al., 2004; Gomez et al., 2006), wastewater sludge (Cai et al., 2004; Wang et al., 2019), agricultural lignocellulosic biomasses (Kumar et al., 2015; Motte et al., 2015; Hu et al., 2018), and agro-food wastes (Buitrón et al., 2014; Mamimin et al., 2016; Ghimire et al., 2017).

The aim of this study was to demonstrate the potential biotechnological valorisation of two biodegradable wastes, cheese whey and orange pulp, which were used as substrates for the DF process to produce H_2 and the required OAs necessary for an efficient ACW treatment. Cheese whey represents approximately 80–90% of the milk used during the

production of cheese and casein and, to date, represents a waste (Colombo et al., 2016). In particular, the global cheese whey production in 2016 was almost equal to 200×10^6 ton y^{-1} and the FAO evaluated a constant 3% increase of cheese whey production in the last 21 years (Domingos et al., 2018). Even if 50% of this by-product is converted into useful products, such as human and animal feed, the rest is disposed of as a waste (Nikodinovic-Runic et al., 2013). Citrus pulp is a waste that is derived from juice-making industries and represents approximately 50% of the processed fruit weight (Mantzouridou and Paraskevopoulou, 2013). The global citrus pulp production may reach 25×10^6 ton y^{-1} (Taghizadeh-Alisaraei et al., 2017), and only a small part of the pulp that is derived from the squeezing of citrus fruits is pelletized and sold for animal feeding (Mamma et al., 2008). Consequently, as in the case of cheese whey, the proposed treatment train could valorise and treat this by-product, which is generally landfilled with a cost that is approximatively equal to 10 USD ton^{-1} (Rossi et al., 2009).

The DF effluents from the biological conversion of orange pulp or cheese whey have been processed with an acid-infused HT treatment to completely dissolve the brucite-like layers of chrysotile fibres and their suspended fragments. In agreement with the findings of a previous work in which sulfuric, malic and lactic acid were tested (Spasiano et al., 2019), in this study, lactic acid was adopted since it seems to be a good compromise in terms of costs, bioavailability, efficiency at dissolving brucitic layers, and bio-methane production during the final AD treatment. However, in this work, oxalic acid was also tested because it costs 50-80% less than lactic acid and it could be considered to be a green chemical. Indeed, oxalic acid could be produced from waste biomasses (André et al., 2010; Musiał et al., 2011) or from the reduction of carbon dioxide (Angamuthu et al., 2010). Additionally, the oxalic acid biodegradation in anaerobic conditions could

generate a methane rich biogas (Dinsdale et al., 2000). Notably, the adoption of oxalic acid instead of lactic or malic acid would both lower the costs of reagents and contribute to the production of methane during the AD of the HT effluents.

The novelty of this work consists in the evaluation of the real feasibility of the proposed process adopting real biodegradable wastes instead of a synthetic glucose solution, which was already tested in our previous papers (Spasiano, 2018; Spasiano et al., 2019). This aspect is crucial because, if the process have to be scaled using glucose as sacrificial biodegradable substrate, the process may not be convenient, or at least less convenient than using agro-food industry wastes. Furthermore, for the first time the evolution of the chrysotile structure degradation has been evaluated at the end of the main steps of the treatment train by means of SEM and EDX analysis.

2. Materials and methods

2.1. Materials

Oxalic acid (≥99%) and lactic acid (85%), which were manufactured by Sigma-Aldrich. The sulfuric acid (98%) in the preparation of the high-pressure liquid chromatography (HPLC) eluent were used. In all of the reported experiments and in the dilution for analytical procedures, demineralized water was adopted as the solvent.

The inoculum that was adopted for the DF experiments was attained by a thermal pretreatment of the digestate, which was derived from an anaerobic digester that was used to treat the wastewater and the biodegradable wastes produced by the dairy farm 'Davide Colangelo', located in southern Italy. In particular, the pretreatment was carried out at 105 °C and lasted 1.0 h (Ghimire et al., 2015). The digestate characterization highlighted the total solids (TS) and volatile solids (VS) at concentrations of 50.3 g L^{-1} and 26.5 g

L^{-1}, respectively, with the initial pH value of 7.8, and finally, the initial dissolved calcium and magnesium concentrations were 276 mg L^{-1} and 626 mg L^{-1}, respectively.

The characterization of the ACW sample that was used in this study, which was reported elsewhere (Spasiano, 2018), showed the presence of chrysotile fibres and Mg^{2+} and Ca^{2+} concentrations that were equal to 3.1 $\%_{w/w}$ and 30.0 $\%_{w/w}$, respectively.

The orange pulp and cheese whey that were adopted in this experimental campaign are characterized by a COD equal to 173.5 g kg^{-1} and 77.5 g L^{-1}, respectively. Additionally, the characterizations of the two substrates, which are reported in Table 1S, agreed with previous findings (Wong et al., 1978; de Moraes Barros et al., 2012). Once received, the substrates were stored at -18 °C, and an orange peel was blended before use to easily manage the specific bio-reactor's feeding procedure.

2.2. Analytical methods

The dissolved magnesium and calcium ion concentrations were measured by flame (acetylene/air) atomic absorption spectrometry (FAAS). Bio-H_2 concentration in the produced biogas was evaluated by Varian Star 3400 gas chromatography (GC). The concentrations of OAs were evaluated by using a HPLC technique. The adopted equipment consisted of an absorbance detector, a gradient pump and a chromatography oven where a cation-exchange column was housed. The solids collected after the DF and HT processes were analysed with a FESEM-EDX electronic microscope after a golden sputtering was carried out with a Sputter Quorum Q150 under Ar atmosphere. The TS, VS, and COD values were measured according to APHA standard methods (Association, 1998). A pH-meter (HI 98190 pH/ORP; Hanna Instruments) was used to monitor the pH of the solutions.

145 Detailed information is presented in the Supporting Materials.

146

147 **2.3. Experimental apparatus**

148 Dark fermentation bioreactors consisted of a 2.0 L borosilicate glass bottle closed with
149 airtight screw caps having two sampling tubes to allow for the withdrawal of liquid and
150 gaseous samples. To guarantee a food to microorganism ratio (F/M), expressed as the
151 COD substrate (g)/VS inoculum (g), close to 2.6 (Spasiano et al., 2017), 500 mL of
152 inoculum was mixed with 407 mL of cheese whey or 182 g of orange pulp. The solutions
153 were made up to the volume of 1.0 L with distilled water and were purged with pure N_2
154 for 30 min to ensure anaerobic conditions. Successively, the bio-reactors were
155 continuously stirred at 370 rpm and maintained at 35 ± 1 °C. The DF experiments were
156 carried out under batch-wise conditions until the cumulative H_2 production reached a
157 plateau to re-activate the inoculum. Later, the stirring of the solution was interrupted for
158 2 h to allow the sedimentation of most of the biomass, and the reactors were fed in fed-
159 batch conditions. In particular, 500 mL of supernatant was removed and replaced by 500
160 mL of a water solution containing 182 g of orange pulp or 407 mL of cheese whey. This
161 procedure was repeated when the cumulative H_2 production reached a plateau for the
162 second time, and 5.0 g of ACW was added to each bioreactor together with the
163 biodegradable substrate.

164 The DF pretreatments of ACW lasted until the cumulative H_2 production reached the
165 plateau for the third time, and the resulting solutions representing the effluent of the DF
166 processes were used for HT experimentation. To this purpose, 100 mL of the afforded
167 solution was heated in a round bottom flask equipped with a glass condenser cooled with
168 tap water (≈15 °C). In particular, the flasks were immersed into an oil bath with a

thermostat at 100 °C and were magnetically stirred. Once the solutions reached the required temperature, oxalic acid or lactic acid was added to the solutions with a concentration in the range of 0–5.0 g L^{-1}. Once withdrawn with a syringe, the samples were centrifuged, filtered, diluted, and, finally, analysed.

3. Results and discussion

3.1. DF treatment

Due to the orange pulp and cheese whey bio-degradation, the H_2 production at the end of the inoculum activation phase (45 h) was 2.6 L and 2.4 L, respectively (Figure 1). This result is in accordance with other studies on DF of real waste biomasses (Kumar et al., 2017; Ghimire et al., 2016) where low H_2 yields and high OA accumulation can be achieved with respect to the case of synthetic glucose-based solutions fermentation. DF of soluble biodegradable compounds, such as sugars, usually lead to the production of acetic acid, butyric acid, propionic acid and ethanol as main by-products (Kumar et al., 2017). The known biological routes for H_2 production usually depend on the bacterial inoculum and substrate characteristics (Ghimire et al., 2016, Ghimire et al., 2017). Due to the complexity of the real-scale derived inoculum and the organic substrates used in this work, the stoichiometry of the process is far to be well known. Based on glucose fermentation by fermentative bacteria (Eq. 1-3 from Costello et al. (1991)), it is possible to assess that the presence of acetic (Eq. 1) and butyric (Eq. 2) acids in the culture medium is more favourable for H_2 production optimization.

$$C_6H_{12}O_6 \rightarrow CH_3CH_2CH_2COOH + 2CO_2 + 2H_2, \quad \text{(Eq. 1)}$$

$$C_6H_{12}O_6 + 2H_2O \rightarrow 2CH_3COOH + 2CO_2 + 4H_2, \quad \text{(Eq. 2)}$$

$$C_6H_{12}O_6 \rightarrow 2CH_3CHOHCOOH. \quad \text{(Eq. 3)}$$

When other fermentation pathways are performed, as in the case of mixed culture-real substrate fermentation, low H_2 yields are achieved and other by-products, such as lactic acid (Eq.3), can be accumulated in the bioreactors. In addition, using high F/M ratios it is possible to favour acids accumulation within the culture medium with uncomplete substrate conversion. This was the aim of DF phase in this work, where high OA concentrations were accumulated for the successive dissolution phase of the ACW treatment. After feeding the bioreactors in semi-batch conditions, the H_2 production decreased. Indeed, with the second and third loads of cheese whey, the H_2 volumes generated in the bioreactor were 2.1 L and 0.5 L, respectively, while lower H_2 volumes were produced by using orange pulp as a biodegradable substrate. This behaviour could be ascribed to the production of other OAs, such as lactic, which led to a decrease in the pH (Figure 2) and the consequent slowdown of bio-H_2 production. Moreover, the lower H_2 production during the DF of orange pulp could be due to the presence of orange peel oil, which was mainly constituted by D-limonene, a monoterpene that is toxic to fermenting microorganisms (Zema et al., 2018). In particular, among the other OAs typically produced during the DF process (Figure 2), the presence of 1468 mg L^{-1} caproic acid at the end of the DF of the orange peel confirms this hypothesis. D-Limonene, by interacting with the membrane structure of specific microorganisms such as *Escherichia coli* and *Salmonella enterica*, led to the change in the membrane lipid profile and to an increase in the caproic acid content to more than 50% (Di Pasqua et al., 2007).

The inhibitory effect of D-limonene also affected the amount and the speciation of produced OAs during the DF. This aspect is highly relevant because inorganic trace elements can add additional inhibitory effects on microbial consortia operating in anaerobic conditions (Maharaj et al., 2018). Indeed, when cheese whey was used as the

217 substrate, the final amount of OAs was higher than when using orange pulp as feedstock.
218 Specifically, the molar ratio among butyric acid and acetic acid (B/A) in the effluents of
219 the last cycle was 1.21, which is a value that is close to the optimal B/A ratio (1.5) that
220 was previously evaluated (Hawkes et al., 2007). On the other hand, during the DF of
221 orange peel, the OA production decreased by almost 40%, and the B/A ratio at the end of
222 the biological phase was also equal to 0.66. These results are higly relevant as they can
223 be used as experimental base for the understanding of the biochemical behaviour of mixed
224 culture consortia and the definition of mathematical models (Frunzo et al., 2019; Mattei
225 et al., 2018; Kostrytsia et al., 2018).
226 However, in both cases, the OAs produced during the DF phase attached the calcium and
227 magnesium compounds contained in the ACW sample that was added 100 h after the
228 beginning of the experiments. Indeed, as shown in Figure 3, most of the Ca-based
229 compounds that constituted the cement matrix of the ACW sample were dissolved, since
230 90% of the theoretical Ca amount in the suspended ACW was found dissolved as Ca^{2+} in
231 both of the effluents of the biological phase. This results is in agreement with the
232 biogeochemical mechanisms of deterioration of concrete due to the metabolic activity of
233 some microorganisms, which leads to the production of OAs that facilitate the calcium
234 complexation and dissolution (Sand, 1997; Jia et al., 2019). Specifically, this
235 phenomenon can contribute to the biodeterioration of cement pipe in drinking water
236 distribution systems (Wang et al., 2011), of buildings and monuments (Dyer, 2017).
237 At the same time, 41.5% and 36.4% of the magnesium constituting the brucitic layer of
238 white asbestos contained in the ACW was found to be dissolved in the DF effluents from
239 cheese whey and orange peel, respectively. Also in this case, the dissolution of the brucitic
240 layer could be ascribed to the metal extracting action of the OAs produced during the DF.

241 Indeed, a similar biodeterioration mechanism was observed in the environment on
242 asbestos and asbestiform minerals exposed to the action of some organisms (bacteria,
243 fungi and lichens), whose metabolites with acidic and chelating functions (such as, oxalic
244 acid, pulvinic and norstictic acid) attack and extract metals from the asbestos structure
245 (Favero-Longo et al., 2013; Mohanty et al., 2018).
246 In particular, as shown in Figure 3, the net concentration of calcium and magnesium ions
247 ($[Ca^{2+}]_n$ and $[Mg^{2+}]_n$) at the end of the DF was normalized with respect to the
248 theoretical calcium and magnesium concentration suspended in the solid state after the
249 addition of 5 g L^{-1} ACW ($[Mg^{2+}]_t$ and $[Ca^{2+}]_t$) as follows:

250 $$\frac{[Mg^{2+}]_n}{[Mg^{2+}]_t} = \frac{[Mg^{2+}]_{171h} - [Mg^{2+}]_{100h}}{155\ mg\ L^{-1}} \quad \text{(Eq. 4)}$$

251 $$\frac{[Ca^{2+}]_n}{[Ca^{2+}]_t} = \frac{[Ca^{2+}]_{171h} - [Ca^{2+}]_{100h}}{1500\ mg\ L^{-1}} \quad \text{(Eq. 5)}$$

252 where $[Mg^{2+}]_{171h}$ and $[Ca^{2+}]_{171h}$ represent the concentrations of dissolved cations at
253 the end of the biological pretreatments, while $[Mg^{2+}]_{100h}$ and $[Ca^{2+}]_{100h}$ are the
254 concentration of the ions dissolved in the solutions just before the 5 g L^{-1} ACW addition.
255 Even when a partial dissolution of the brucitic layers was observed in both cases,
256 asbestos-like fibres were still present. Indeed, SEM analysis carried out on the suspended
257 solids contained in the DF effluents showed some fibres that were characterized by a
258 morphology that is very similar to that of chrysotile (Figure 1S). In agreement with the
259 lower amount of dissolved magnesium, the fibres found in the effluents of the DF that
260 were carried out in the presence of orange peel (Figures 1Sc-d) seemed larger than in the
261 other case. Additionally, the EDX analysis carried out on the fibres (sites S1-S6 of Figure
262 1S) revealed an Mg/Si weight ratio that was close to the theoretical Mg/Si ratio of pure

chrysotile (1.298 g_{Mg}/g_{Si}). Indeed, the Mg/Si ratios were all in the range of 1.185-1.017 g_{Mg}/g_{Si}, except in the case of a thin fibre (site S4) that had a Mg/Si ratio of 0.814 g_{Mg}/g_{Si}. Most likely, the attack of the OAs produced during the DF begins with the defibration of the chrysotile and the consequent generation of increasingly thinner bundles of fibrils. Due to the larger specific surface area, the latter may be attacked faster by the OAs, with a consequent decrease in the Mg/Si ratio. Although the Mg/Si ratios were lower than the theoretical value and the chrysotile fibres seemed to have suffered an alteration, an HT treatment should be carried out.

3.2. Acid-infused hydrothermal treatment

To ensure the collapse of all the residual chrysotile fibres in the effluents of the biological pretreatment, HT treatment tests were carried out at 100 °C under ambient pressure. In particular, the effects of lactic and oxalic acid additions during the HT treatment of the DF effluents were investigated. As reported in Figure 4, a slight effect of the acid type was observed during the tests. Indeed, higher magnesium concentrations were detected at the beginning of the experiments, when oxalic acid was used instead of lactic acid. Since the two organic acids used in this study are characterized by the same molecular weight, using the same loading condition for each specific HT test caused the molar concentrations to coincide. Consequently, the different efficiencies of the adopted acids could be ascribed to the acidity and the chelating properties of the two compounds. Oxalic acid has pK_a values equal to 1.25 and 4.14 (Faria et al., 2008), while the pK_a value of lactic acid is 3.86 (Luongo et al., 2019; Gonzalez et al., 2008). Additionally, oxalic acid has more pronounced chelating properties than lactic acid due to the presence of two carboxylic groups.

Apart from the different hydrogen productions, the biodegradable substrates that were added during the DF pretreatment also play a key role in the HT step. Indeed, when cheese whey was used, the HT treatments of the DF effluents (Figure 4a) result in a more efficient brucitic sheet dissolution with respect to the treatment of the DF effluents carried out by using orange peel as the biodegradable substrate (Figure 4b). Indeed, with the addition of 1.25 g L^{-1} lactic acid or oxalic acid to the effluents of the DF carried out with cheese whey, almost 91% of brucitic sheets dissolution was achieved after 12 h of HT treatment at 100 °C. On the other hand, when orange peel was used as the substrate, with the addition of the same loads of lactic and oxalic acid, almost 87% of brucite-like sheets were dissolved. These results are probably due to the high amount of OAs produced during the DF process: the more OAs are produced during the DF treatment, the higher is the dissolution efficiency of the brucitic sheets at the end of both the DF and HT treatments (Table 1).

Regardless of the biodegradable substrate that was used during the DF, no chrysotile-like fibres were found during the SEM analysis of the solids that were withdrawn at the end of the HT processes carried out with the addition of 5.0 g L^{-1} and 2.5 g L^{-1} lactic acid. On the other hand, SEM analysis of the suspended solids collected after the HT process was carried out with the addition of only 1.25 g L^{-1} lactic acid showed the presence of few small fibres, which were similar to chrysotile. These fibrils, which are shown in Figure 2S, were smaller and thinner than those found in the DF effluents that are shown in Figure 1S. Moreover, the Mg/Si weight ratios of the fibrils indicates strong damage to the brucitic layer. Indeed, the EDX analysis carried out on these fibre fragments (sites S7-S10 of Figure 2S) highlighted the Mg/Si ratios in the range of 0.86 g_{Mg}/g_{Si} (site S9) to 0.52 g_{Mg}/g_{Si} (site S7).

311 Even if most of the chrysotile fibres collapsed and their fragments have a chemical
312 composition that is different from that of white asbestos, the addition of 1.25 g L^{-1} lactic
313 acid or, supposedly, oxalic acid, may not guarantee the complete destruction of all of the
314 asbestos fibres. Moreover, there is no information about the toxicity of the fragments that
315 are shown in Figure 2S. Consequently, it would be advisable to extend the duration of the
316 treatment or to increase the concentrations of acids to avoid any environmental issues that
317 are related to the treatment train.
318

319 ## 4. Conclusion

320 The DF of orange pulp and cheese whey resulted in an effective pretreatment for the acid-infused
321 HT phase of ACWs. Indeed, the biological treatment of these two agro-food wastes led to the
322 production of OAs and H_2, which can reduce the reagent and energy costs of the HT treatment.
323 In comparison with the DF of orange pulp, which is rich in D-limonene, higher H_2 and organic
324 acid production rates were observed when the cheese whey was used as the substrate. In both
325 cases, the addition of 2.5 g L^{-1} lactic or oxalic acid, before an HT treatment lasting 12 h, allowed
326 for the effective treatment of 5 g L^{-1} ACW. On the other hand, when lactic and oxalic acid were
327 added at the concentration of 1.25 g L^{-1}, a few fibre fragments were found in HT effluents, and
328 their chemical composition differed from that of chrysotile.
329

330 ## Acknowledgement

331 The Authors thank Prof. Paolo Calabrò and Prof. Luigi Frunzo for providing the
332 biodegradable substrates and for technical support.
333
334

335 **References**

336 André, A., Diamantopoulou, P., Philippoussis, A., Sarris, D., Komaitis, M.,
337 Papanikolaou, S., 2010. Biotechnological conversions of bio-diesel
338 derived waste glycerol into added-value compounds by higher fungi:
339 production of biomass, single cell oil and oxalic acid. Ind. Crops Prod.
340 31, 407–416.

341 Angamuthu, R., Byers, P., Lutz, M., Spek, A.L., Bouwman, E., 2010.
342 Electrocatalytic CO_2 conversion to oxalate by a copper complex.
343 Science (80-.). 327, 313–315.

344 Association, A.P.H., 1998. APHA. 1998. Stand. methods Exam. water
345 wastewater 20.

346 Buitrón, G., Prato-Garcia, D., Zhang, A., 2014. Biohydrogen production
347 from tequila vinasses using a fixed bed reactor. Water Sci. Technol. 70,
348 1919–1925.

349 Cai, M., Liu, J., Wei, Y., 2004. Enhanced biohydrogen production from
350 sewage sludge with alkaline pretreatment. Environ. Sci. Technol. 38,
351 3195–3202.

352 Colombo, B., Sciarria, T.P., Reis, M., Scaglia, B., Adani, F., 2016.
353 Polyhydroxyalkanoates (PHAs) production from fermented cheese
354 whey by using a mixed microbial culture. Bioresour. Technol. 218, 692–
355 699.

356 Costello, D.J., Greenfield, P.F. and Lee, P.L., 1991. Dynamic modelling of
357 a single-stage high-rate anaerobic reactor—I. Model derivation. Water
358 research 25(7), 847–858.
359 De Moraes Barros, H.R., de Castro Ferreira, T.A.P., Genovese, M.I., 2012.
360 Antioxidant capacity and mineral content of pulp and peel from
361 commercial cultivars of citrus from Brazil. Food Chem. 134, 1892–
362 1898.
363 Di Pasqua, R., Betts, G., Hoskins, N., Edwards, M., Ercolini, D., Mauriello,
364 G., 2007. Membrane toxicity of antimicrobial compounds from essential
365 oils. J. Agric. Food Chem. 55, 4863–4870.
366 Dinsdale, R.M., Hawkes, F.R., Hawkes, D.L., 2000. Anaerobic digestion of
367 short chain organic acids in an expanded granular sludge bed reactor.
368 Water Res. 34, 2433–2438.
369 Domingos, J.M., Puccio, S., Martinez, G.A., Amaral, N., Reis, M.A.M.,
370 Bandini, S., Fava, F., Bertin, L., 2018. Cheese whey integrated
371 valorisation: Production, concentration and exploitation of carboxylic
372 acids for the production of polyhydroxyalkanoates by a fed-batch
373 culture. Chemical Engineering Journal, 336, 47–53.
374 Donaldson, K., Poland, C.A., Murphy, F.A., MacFarlane, M., Chernova, T.,
375 Schinwald, A., 2013. Pulmonary toxicity of carbon nanotubes and

376 asbestos—similarities and differences. Adv. Drug Deliv. Rev. 65, 2078–
377 2086.
378 Dyer, T., 2017. Deterioration of stone and concrete exposed to bird excreta–
379 Examination of the role of glyoxylic acid. International Biodeterioration
380 & Biodegradation 125, 125–141.
381 Falini, G., Foresti, E., Gazzano, M., Gualtieri, A.F., Leoni, M., Lesci, I.G.,
382 Roveri, N., 2004. Tubular-Shaped Stoichiometric Chrysotile
383 Nanocrystals. Chem. Eur. J. 10, 3043–3049.
384 Faria, P.C.C., Órfão, J.J.M., Pereira, M.F.R., 2008. Activated carbon
385 catalytic ozonation of oxamic and oxalic acids. Appl. Catal. B Environ.
386 79, 237–243.
387 Favero-Longo, S.E., Turci, F., Fubini, B., Castelli, D., Piervittori, R., 2013.
388 Lichen deterioration of asbestos and asbestiform minerals of serpentinite
389 rocks in Western Alps. International Biodeterioration & Biodegradation
390 84, 342–350.
391 Frunzo, L., Fermoso, F.G., Luongo, V., Mattei, M.R., Esposito, G., 2019.
392 ADM1-based mechanistic model for the role of trace elements in
393 anaerobic digestion processes. J. Environ. Manage. 241, 587–602.
394 Ghimire, A., Frunzo, L., Pontoni, L., d'Antonio, G., Lens, P.N.L., Esposito,
395 G., Pirozzi, F., 2015. Dark fermentation of complex waste biomass for

biohydrogen production by pretreated thermophilic anaerobic digestate. J. Environ. Manage. 152, 43–48.

Ghimire, A., Sposito, F., Frunzo, L., Trably, E., Escudié, R., Pirozzi, F., Lens, P.N., Esposito, G., 2016. Effects of operational parameters on dark fermentative hydrogen production from biodegradable complex waste biomass. Waste Manag. 50, 55–64.

Ghimire, A., Luongo, V., Frunzo, L., Pirozzi, F., Lens, P.N.L., Esposito, G., 2017. Continuous biohydrogen production by thermophilic dark fermentation of cheese whey: Use of buffalo manure as buffering agent. Int. J. Hydrogen Energy 42, 4861–4869.

Gomez, X., Moran, A., Cuetos, M.J., Sanchez, M.E., 2006. The production of hydrogen by dark fermentation of municipal solid wastes and slaughterhouse waste: a two-phase process. J. Power Sources 157, 727–732.

Gonzalez, M.I., Alvarez, S., Riera, F.A., Alvarez, R., 2008. Lactic acid recovery from whey ultrafiltrate fermentation broths and artificial solutions by nanofiltration. Desalination 228, 84–96.

Hawkes, F.R., Hussy, I., Kyazze, G., Dinsdale, R., Hawkes, D.L., 2007. Continuous dark fermentative hydrogen production by mesophilic microflora: principles and progress. Int. J. Hydrogen Energy 32, 172–184.

417 Hu, B.-B., Li, M.-Y., Wang, Y.-T., Zhu, M.-J., 2018. High-yield
418 biohydrogen production from non-detoxified sugarcane bagasse:
419 Fermentation strategy and mechanism. Chem. Eng. J. 335, 979–987.
420 Jia, R., Unsal, T., Xu, D., Lekbach, Y., Gu, T., 2019. Microbiologically
421 influenced corrosion and current mitigation strategies: A state of the art
422 review. International Biodeterioration & Biodegradation 137, 42–58.
423 Kostrytsia, A., Papirio, S., Frunzo, L., Mattei, M.R., Porca, E., Collins, G.,
424 Lens, P.N., Esposito, G., 2018. Elemental sulfur-based autotrophic
425 denitrification and denitritation: microbially catalyzed sulfur hydrolysis
426 and nitrogen conversions. J. Environ. Manage. 211, 313–322.
427 Kumar, G., Bakonyi, P., Periyasamy, S., Kim, S.H., Nemestóthy, N., Bélafi-
428 Bakó, K., 2015. Lignocellulose biohydrogen: practical challenges and
429 recent progress. Renew. Sustain. Energy Rev. 44, 728–737.
430 Kumar, G., Sivagurunathan, P., Pugazhendhi, A., Thi, N.B.D., Zhen, G.,
431 Chandrasekhar, K., Kadier, A., 2017. A comprehensive overview on
432 light independent fermentative hydrogen production from wastewater
433 feedstock and possible integrative options. Energy conversion and
434 management 141, 390–402.
435 Luongo, V., Palma, A., Rene, E.R., Fontana, A., Pirozzi, F., Esposito, G. and
436 Lens, P.N., 2019. Lactic acid recovery from a model of Thermotoga
437 neapolitana fermentation broth using ion exchange resins in batch and

438 fixed-bed reactors. Separation Science and Technology 54(6), 1008–
439 1025.
440 Maharaj, B.C., Mattei, M.R., Frunzo, L., van Hullebusch, E.D. and Esposito,
441 G., 2018. ADM1 based mathematical model of trace element
442 precipitation/dissolution in anaerobic digestion processes. Bioresour.
443 Technol. 267, 666–676.
444 Mamimin, C., Jehlee, A., Saelor, S., Prasertsan, P., Sompong, O., 2016.
445 Thermophilic hydrogen production from co-fermentation of palm oil
446 mill effluent and decanter cake by Thermoanaerobacterium
447 thermosaccharolyticum PSU-2. Int. J. Hydrogen Energy 41, 21692–
448 21701.
449 Mamma, D., Kourtoglou, E., Christakopoulos, P., 2008. Fungal
450 multienzyme production on industrial by-products of the citrus-
451 processing industry. Bioresour. Technol. 99, 2373–2383.
452 Mantzouridou, F., Paraskevopoulou, A., 2013. Volatile bio-ester production
453 from orange pulp-containing medium using Saccharomyces cerevisiae.
454 Food Bioprocess Technol. 6, 3326–3334.
455 Mattei, M.R., Frunzo, L., D'acunto, B., Pechaud, Y., Pirozzi, F., Esposito,
456 G., 2018. Continuum and discrete approach in modeling biofilm
457 development and structure: a review. Journal of Mathematical Biology
458 76(4), 945–1003.

459 Mohanty, S.K., Gonneau, C., Salamatipour, A., Pietrofesa, R.A., Casper, B.,
460 Christofidou-Solomidou, M., Willenbring, J.K., 2018. Siderophore-
461 mediated iron removal from chrysotile: Implications for asbestos
462 toxicity reduction and bioremediation. J. Hazard. Mater. 341, 290–296.
463 Motte, J.-C., Sambusiti, C., Dumas, C., Barakat, A., 2015. Combination of
464 dry dark fermentation and mechanical pretreatment for lignocellulosic
465 deconstruction: an innovative strategy for biofuels and volatile fatty
466 acids recovery. Appl. Energy 147, 67–73.
467 Musiał, I., Cibis, E., Rymowicz, W., 2011. Designing a process of kaolin
468 bleaching in an oxalic acid enriched medium by Aspergillus niger
469 cultivated on biodiesel-derived waste composed of glycerol and fatty
470 acids. Appl. Clay Sci. 52, 277–284.
471 Nam, S.-N., Jeong, S., Lim, H., 2014. Thermochemical destruction of
472 asbestos-containing roofing slate and the feasibility of using recycled
473 waste sulfuric acid. J. Hazard. Mater. 265, 151–157.
474 Nikodinovic-Runic, J., Guzik, M., Kenny, S.T., Babu, R., Werker, A.,
475 Connor, K.E.O., 2013. Carbon-rich wastes as feedstocks for
476 biodegradable polymer (polyhydroxyalkanoate) production using
477 bacteria, in: Advances in Applied Microbiology. Elsevier, pp. 139–200.
478 OVAM, n.d. State of the art: asbestos - Possible treatment methods in
479 Flanders: constraints and opportunities. 2016.

480 Plescia, P., Gizzi, D., Benedetti, S., Camilucci, L., Fanizza, C., De Simone,
481 P., Paglietti, F., 2003. Mechanochemical treatment to recycling
482 asbestos-containing waste. Waste Manag. 23, 209–218.
483 Rossi, S.C., Vandenberghe, L.P.S., Pereira, B.M.P., Gago, F. D., Rizzolo,
484 J.A., Pandey, A., Soccol, C.R., Medeiros, A.B.P. (2009). Improving
485 fruity aroma production by fungi in SSF using citric pulp. Food Research
486 International, 42(4), 484–486.
487 Saleem, M., Lavagnolo, M.C., Spagni, A., 2018. Biological hydrogen
488 production via dark fermentation by using a side-stream dynamic
489 membrane bioreactor: Effect of substrate concentration. Chem. Eng. J.
490 349, 719–727.
491 Sand, W., 1997. Microbial mechanisms of deterioration of inorganic
492 substrates—a general mechanistic overview. International
493 Biodeterioration & Biodegradation 40(2-4), 183–190.
494 Sen, K.Y., Hussin, M.H., Baidurah, S., 2019. Biosynthesis of poly (3-
495 hydroxybutyrate)(PHB) by Cupriavidus necator from various pretreated
496 molasses as carbon source. Biocatalysis and Agricultural
497 Biotechnology, 17, 51–59.
498 Shin, H.-S., Youn, J.-H., Kim, S.-H., 2004. Hydrogen production from food
499 waste in anaerobic mesophilic and thermophilic acidogenesis. Int. J.
500 Hydrogen Energy 29, 1355–1363.

501 Spasiano, D., 2018. Dark fermentation process as pretreatment for a
502 sustainable denaturation of asbestos containing wastes. J. Hazard.
503 Mater. 349, 45–50.
504 Spasiano, D., Luongo, V., Petrella, A., Alfè, M., Pirozzi, F., Fratino, U.,
505 Piccinni, A.F., 2017. Preliminary study on the adoption of dark
506 fermentation as pretreatment for a sustainable hydrothermal
507 denaturation of cement-asbestos composites. J. Clean. Prod. 166, 172–
508 180.
509 Spasiano, D., Luongo, V., Race, M., Petrella, A., Fiore, S., Apollonio, C.,
510 Pirozzi, F., Fratino, U., Piccinni, A.F., 2019. Sustainable bio-
511 hydrothermal sequencing treatment for asbestos-cement wastes. J.
512 Hazard. Mater. 364, 256-263.
513 Spasiano, D., Pirozzi, F., 2017. Treatments of asbestos containing wastes. J.
514 Environ. Manage. 204, 82–91.
515 Stayner, L., Welch, L.S., Lemen, R., 2013. The worldwide pandemic of
516 asbestos-related diseases. Annu. Rev. Public Health 34, 205–216.
517 Taghizadeh-Alisaraei, A., Hosseini, S.H., Ghobadian, B., Motevali, A.,
518 2017. Biofuel production from citrus wastes: A feasibility study in Iran.
519 Renewable and Sustainable Energy Reviews, 69, 1100–1112.

520 Wang, D., Cullimore, R., Hu, Y., Chowdhury, R., 2011. Biodeterioration of
521 asbestos cement (AC) pipe in drinking water distribution systems.
522 International Biodeterioration & Biodegradation 65(6), 810–817.
523 Wang, D., Zhang, D., Xu, Q., Liu, Y., Wang, Q., Ni, B.-J., Yang, Q., Li, X.,
524 Yang, F., 2019. Calcium peroxide promotes hydrogen production from
525 dark fermentation of waste activated sludge. Chem. Eng. J. 355, 22–32.
526 Wong, N.P., LaCroix, D.E., McDonough, F.E., 1978. Minerals in whey and
527 whey fractions. J. Dairy Sci. 61, 1700–1703.
528 Zema, D.A., Fòlino, A., Zappia, G., Calabrò, P.S., Tamburino, V., Zimbone,
529 S.M., 2018. Anaerobic digestion of orange peel in a semi-continuous
530 pilot plant: An environmentally sound way of citrus waste management
531 in agro-ecosystems. Science of The Total Environment, 630, 401–408.
532

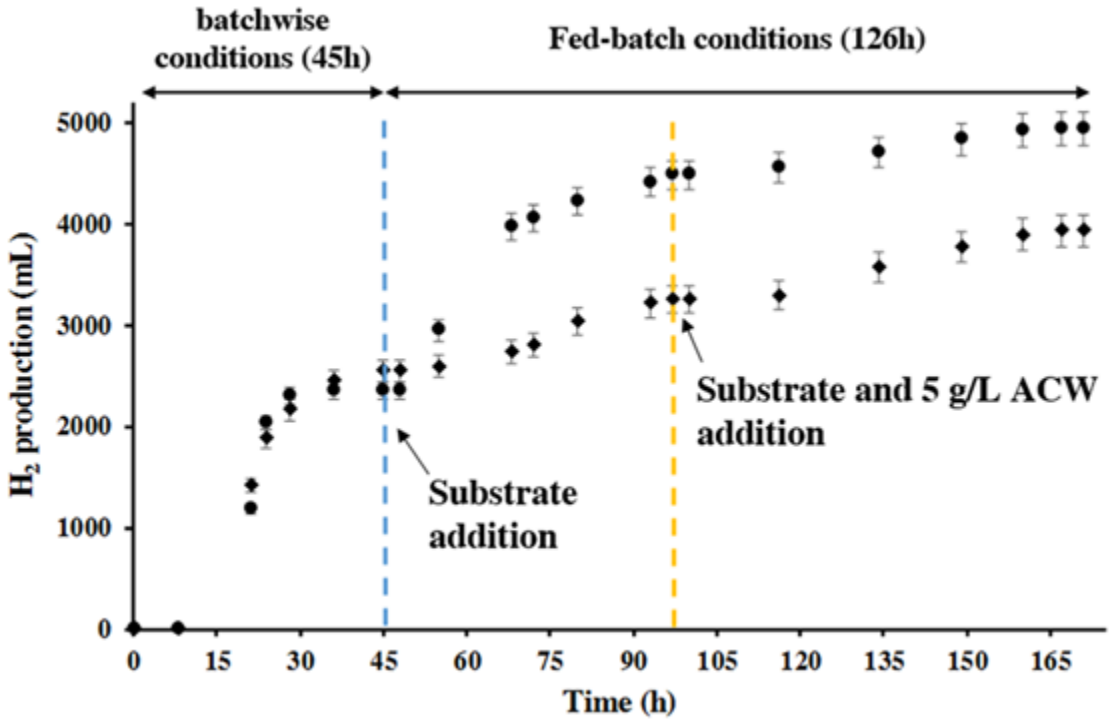

Figure 1. Bio-H_2 production during the DF process by using orange pulp (♦) and cheese whey (●) as biodegradable substrates. V_{sol} = 1.0 L. $[ACW]_{100h}$ = 5 g L^{-1}. T = 35 °C.

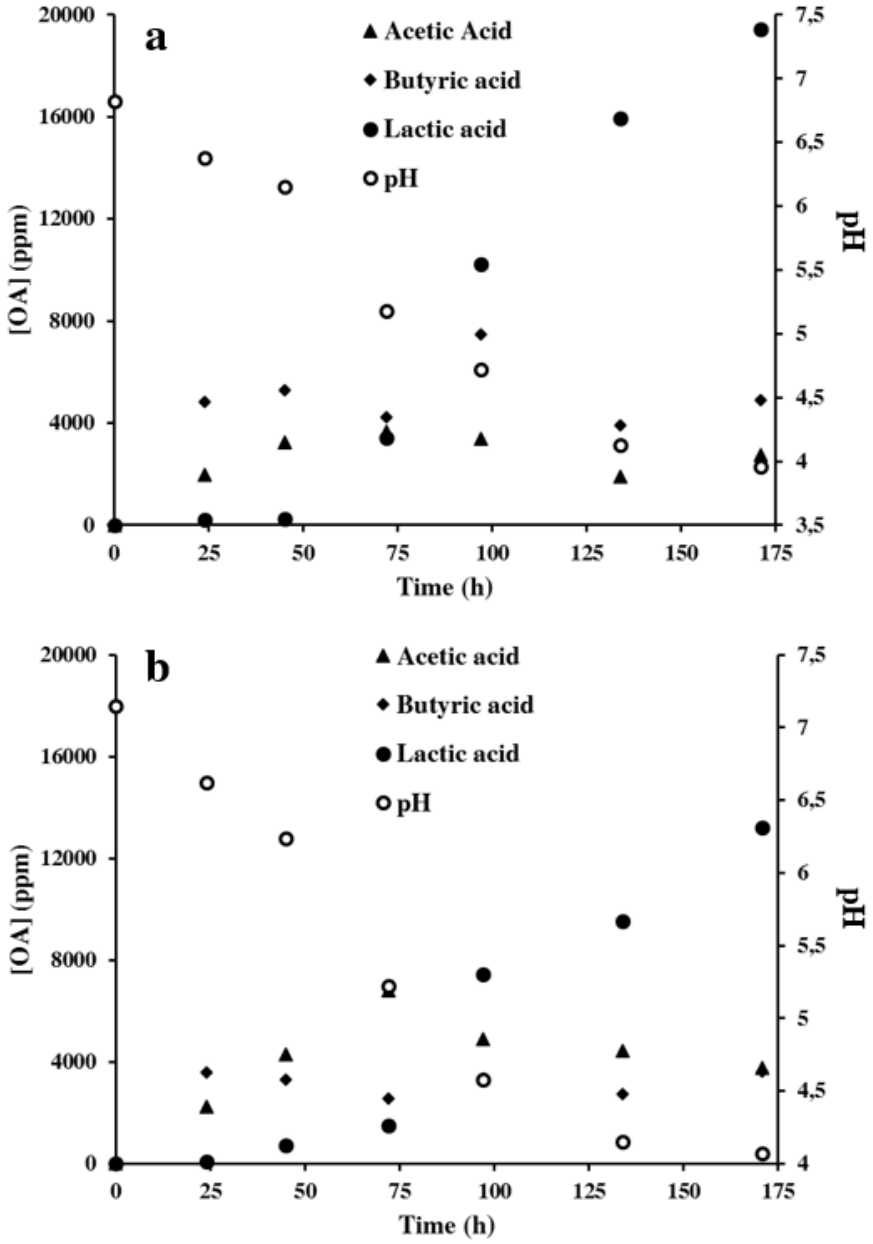

Figure 2. Monitoring of OA production and the pH trend during the DF treatment carried out in the presence of cheese whey (a) and orange pulp (b). V_{sol} = 1.0 L. $[ACW]_{100h}$ = 5 g L^{-1}. T = 35 °C.

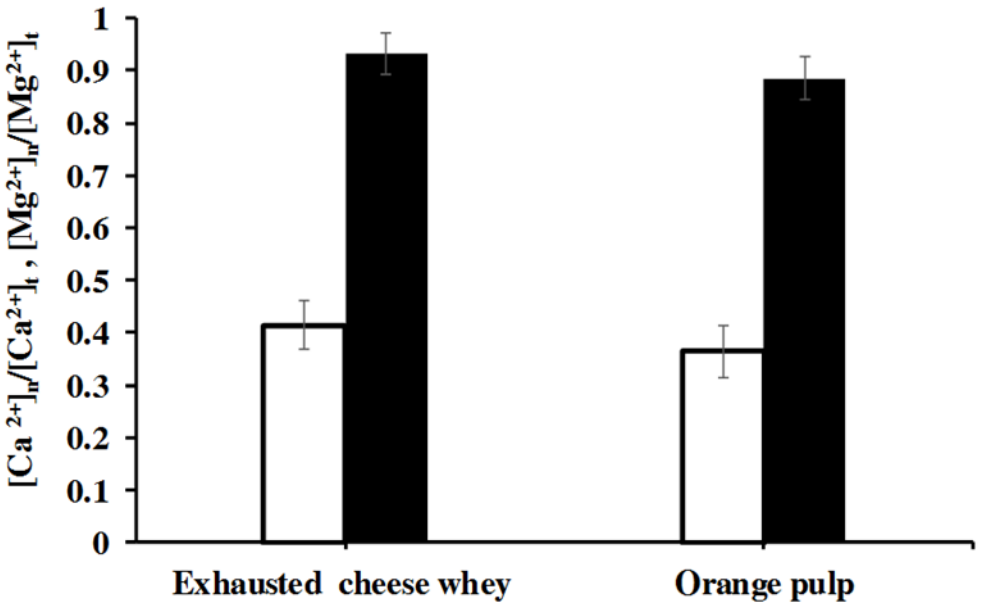

Figure 3. Net normalized magnesium and calcium concentration at the end of the DF process. V_{sol} = 1.0 L. $[ACW]_{100h}$ = 5 g L^{-1}. T = 35 °C.

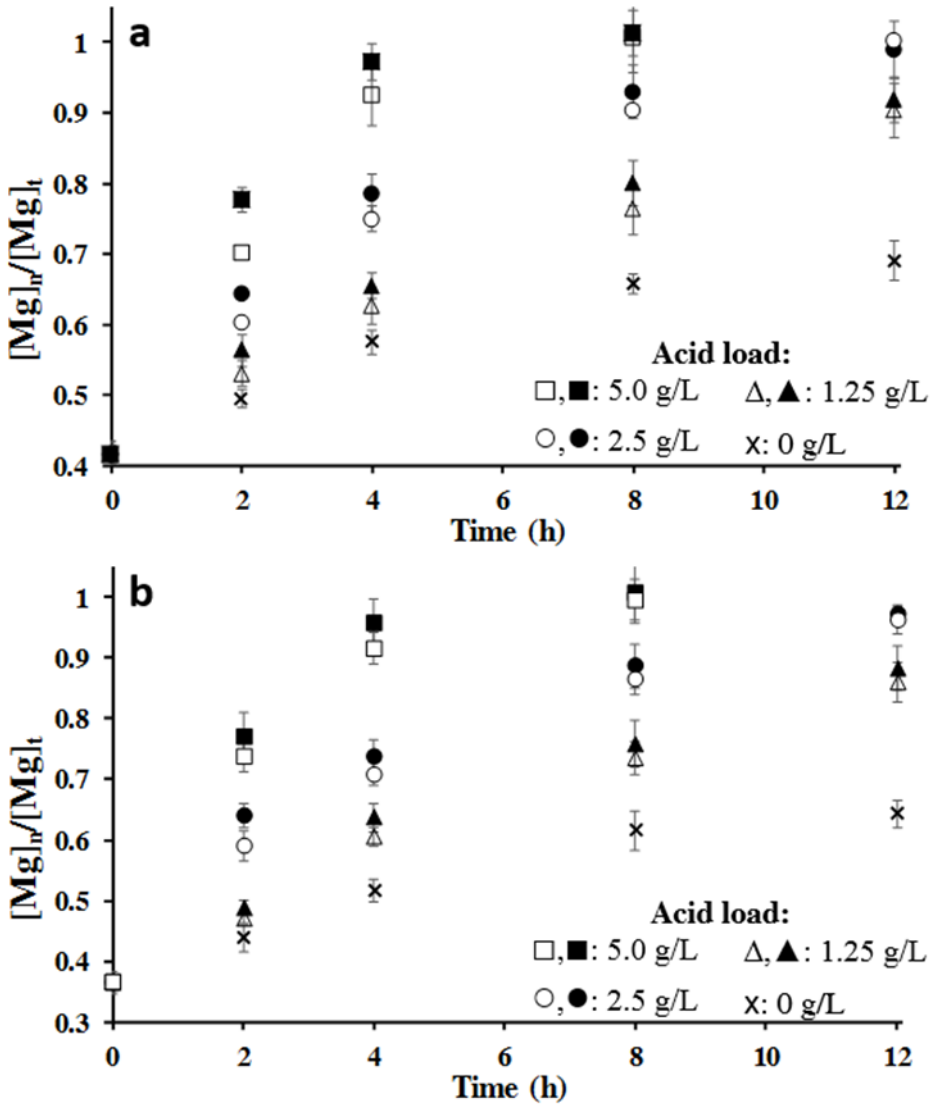

Figure 4. Effect of lactic acid (empty symbols) and oxalic acid (full symbols) loads on the HT treatment of the effluents deriving from the DF of cheese whey (a) and orange peel (b).

	Cheese whey	Orange peel	Glucose[a]
[Butyric acid] (mM)	55.5	41.1	188.3
[Acetic acid] (mM)	45.6	62.7	38.5
[Lactic acid] (mM)	215.7	146.8	119.8
$[Mg]_n/[Mg]_t$ before the HT treatment	0.41	0.36	0.48
$[Mg]_n/[Mg]_t$ after 12 h HT treatment (T=100 °C; 1.25 g L^{-1} lactic acid addition)	0.90	0.86	0.93

Table 1. Effect of the biodegradable substrate on the production and speciation of OAs and on the brucite-like layer dissolution. [a] Data reported in a previous study (Spasiano et al., 2019).

Conflict of Interest and Authorship Conformation Form

Please check the following as appropriate:

- ☒ All authors have participated in (a) conception and design, or analysis and interpretation of the data; (b) drafting the article or revising it critically for important intellectual content; and (c) approval of the final version.
- ☒ This manuscript has not been submitted to, nor is under review at, another journal or other publishing venue.
- ☒ The authors have no affiliation with any organization with a direct or indirect financial interest in the subject matter discussed in the manuscript
- ○ The following authors have affiliations with organizations with direct or indirect financial interest in the subject matter discussed in the manuscript:

Corresponding Author's name	Affiliation	Signature
Danilo Spasiano	Polytechnic of Bari	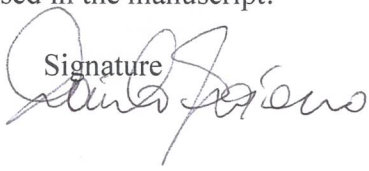

Supplementary materials

a) Analytical methods

The dissolved magnesium and calcium ion concentrations were measured by flame (acetylene/air) atomic absorption spectrometry (FAAS). For this purpose, a Varian Model 55B SpectrAA having a deuterium lamp for background correction was used.

Bio-H_2 concentration in the produced biogas was evaluated by gas chromatography (GC). For this purpose, a Varian Star 3400 equipped with a ShinCarbon ST 80/100 column and a thermal conductivity detector was used, adopting pure Ar as the carrier gas.

The concentrations of OAs were evaluated using a high-pressure liquid chromatography (HPLC) technique. The adopted equipment consisted of a Dionex AD25 absorbance detector, a Dionex GP 50bgradient pump and a Dionex LC 25 chromatography oven where a Metrohm Metrosep Organic Acids – 250/7.8 column was housed. The eluent adopted during the analysis was a solution containing 0.5 mM sulfuric acid, and it was pumped at a flow rate of 0.7 mL/min.

The solids collected after the DF and HT processes were analysed with a FESEM-EDX Carl Zeiss Sigma 300 VP electronic microscope after a golden sputtering carried out with a Sputter Quorum Q150 under Ar atmosphere. In particular, the analysed solids were obtained from ≈25 mL of suspension, which was dehydrated by means of a Martin Christ Alpha 1-4 LSCplus lyophilizer.

The TS, VS, and COD values were measured according to APHA standard methods (APHA, 1998). A pH-meter (HI 98190 pH/ORP; Hanna Instruments) was used to monitor the pH of the solutions.

b) Supplementary table

	[TS]	[VS]	[COD]	[Ca]	[Mg]
Orange pulp[a]	190	183	173.5	810×10^{-3}	258×10^{-3}
Cheese whey[b]	62	59	77.5×10^{3}	1061	248

Table 1S. Orange pulp and cheese whey characterization. [a] Results are reported in g kg^{-1} of fresh weight. [b] Results are reported in mg L^{-1}.

c) Supplementary Figures

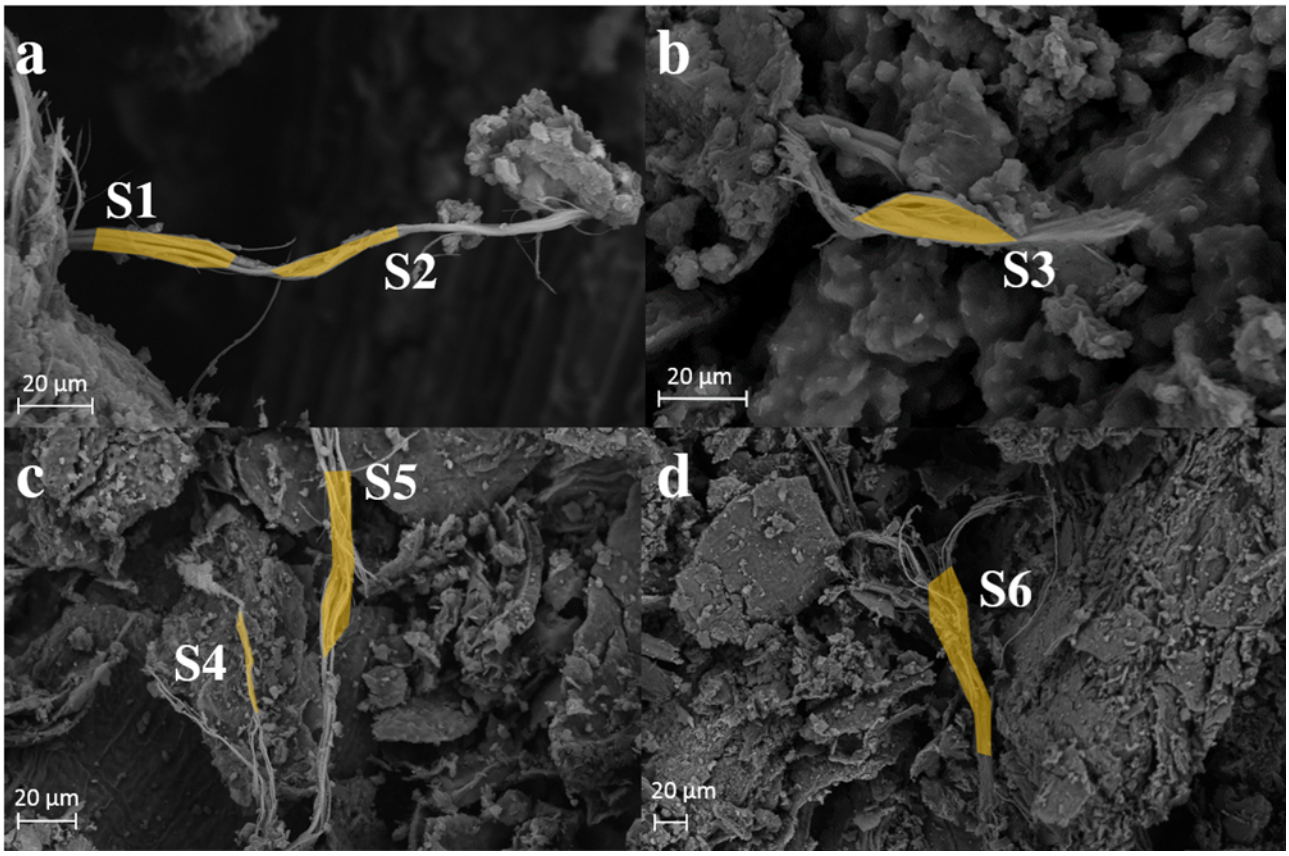

Figure 1S. SEM images of the suspension withdrawal after the DF step was carried out with cheese whey (a-b) and orange pulp (c-d). The highlighted parts represent the areas where the EDX analyses were performed.

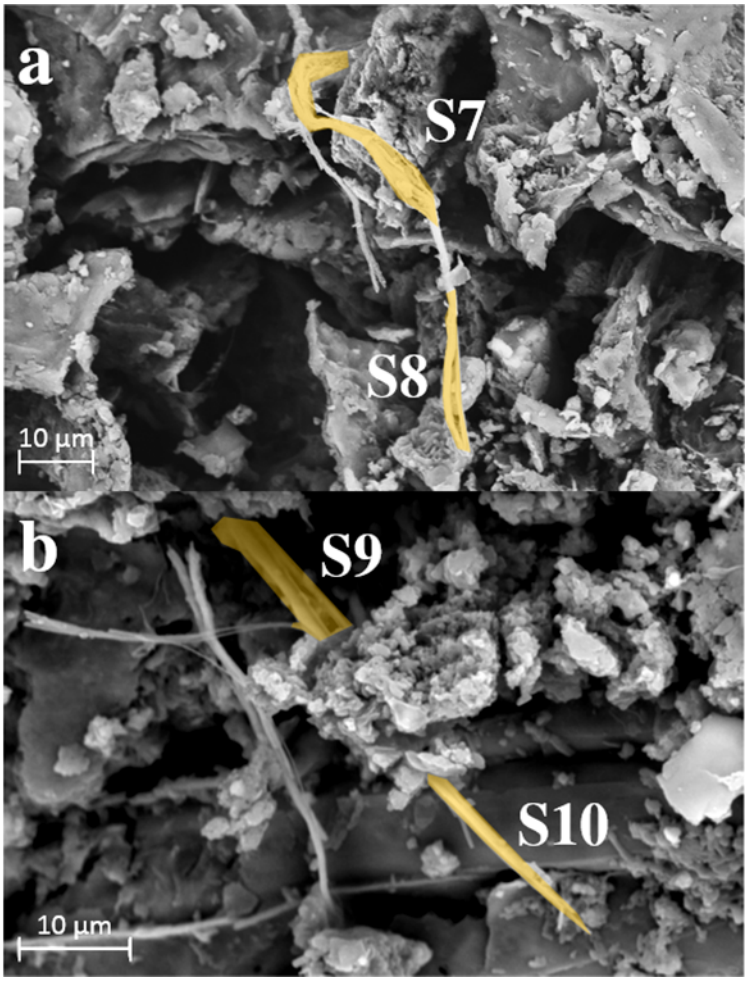

Figure 2S. SEM images of the suspension withdrawal after the HT treatment (1.25 g/L lactic acid) of the effluents of the DF, carried out with orange pulp (a) and cheese whey (b). The highlighted sites represent areas where EDX analyses were performed.